On the Application of Photoacoustic Absorption Spectral Data to the Modeling of Leaf Optical Properties

by

Denise Eng

A thesis
presented to the University of Waterloo
in fulfillment of the
thesis requirement for the degree of
Master of Mathematics
in
Computer Science

Waterloo, Ontario, Canada, 2007

Declaration

I hereby declare that I am the sole author of this thesis. This is a true copy of the thesis, including any required final revisions, as accepted by my examiners.

I understand that my thesis may be made electronically available to the public.

Abstract

Due to the importance of plants in the Earth's ecosystem, their photobiological responses have become the subject of extensive research in life sciences. Leaf optical models have been developed to assist in the analysis of remotely sensed data to derive information on leaf biochemistry and anatomy from foliar spectral curves (transmittance and reflectance). In this paper, we investigate the implications of using *in vitro* pigment absorption spectra to model foliar optical properties in the visible domain. Typically pigment absorption spectra have been determined using light absorption spectroscopy or by applying a data fitting approach. Alternatively, we propose the use of photoacoustic absorption spectroscopy, which despite being available in the literature has not been used in the modeling of foliar optical properties before. We also perform computational experiments in which foliar modeled reflectance and transmittance spectral curves generated using these different absorption data sets are compared with actual measured data. Our findings indicate that the proposed alternative not only allows key pigments to be individually incorporated into the models, which, in turn, increases the predictability of the simulations, but also enables the generation of modeled leaf spectra that are closer approximations to measured leaf spectra than those obtained using absorption data derived from standard absorption spectroscopy procedures.

Acknowledgements

First, I would like to thank Gladimir Baranoski for all of his guidance and support during my research. Both his enthusiasm and valuable advice has made the process of completing this work an extremely rewarding experience. I'd like to thank my readers, Bruce Simpson and Jeff Orchard, for their feedback and suggestions. Special thanks to Francis T. Chen for growing the soybean plant and teaching me how to use the microscope to take digital photos. Finally, I would like to thank my family and friends for their love and support over the last three years.

Contents

List of Tables

List of Figures

Chapter 1

Introduction

Plants play a vital role in the Earth's ecosystem by converting light energy, water and carbon dioxide into organic compounds and oxygen. These byproducts fuel the food chain on which all life depends on, and contribute to the exchange of gases that influence our planet's atmosphere and climate. Consequently, plants have become an important subject of theoretical and applied biological research. In areas such as forestry [37], agriculture [69, 53] and ecology [22], remote sensing has been used to monitor the health and development of crops, trees and other vegetative resources.

The development of predictive, biophysically-based models to simulate the interaction of light with foliar tissues has improved our use of remote sensing data in these applications. Biophysically-based models simulate the propagation of light through organic materials by taking into account the underlying physical processes. By controlling the model with meaningful biophysical parameters, the goal is to

produce reflectance and transmittance spectra that approximates, as closely as possible, the real-world spectra observed for a specimen with the same characteristics. Thus, researchers can obtain valuable information on leaf biochemistry and anatomy from their measured spectra [24]. In order to evaluate the correctness of a leaf optical model, biophysical data obtained from physical experiments is used to set parameter values, and qualitative and quantitative comparisons of modeled leaf spectra are performed with measured leaf spectra. Such evaluations are particularly important if a predictive model is to be used with confidence in other scientific investigations [31]. For example, without comparisons to determine how closely the model approximates real-world behavior, there could be serious consequences for a researcher who uses modeled data as a replacement for physically measured data that is not readily available. For a review of current leaf optical models, we refer the reader to texts by Jacquemoud and Ustin [41] and Baranoski and Rokne [5].

The biophysically-based modeling of leaf optical properties takes into account the absorptive properties of leaf tissue, since it is the scattering of non-absorbed incident light rays that determines leaf reflectance and transmittance. The absorptive properties of leaf tissue can be modeled using the absorptive properties of its individual biochemical constituents, expressed using their specific absorption coefficient (s.a.c.). The specific absorption coefficient of a material is defined as the absorbance of incident light at wavelength λ, per unit path length (usually 1cm) per unit mass concentration (usually g/cm^3 or μg/cm^3) of the material. The light absorption spectrum of a material is simply a plot of its s.a.c. values against the wavelength of incident light.

1.1 Motivation

The initial motivation of this work was to investigate the changes a leaf undergoes due to aging or senescence. Plant senesence can be observed in the fall, when leaves change colour from green to red, yellow and orange. These changes in colour are a result of changes in leaf optical properties, which in turn are due to changes in leaf physiology and biochemistry. However the specific nature of these physiological and biochemical changes are not well-known due to the fact that the methods used to obtain such information are typically destructive, making it extremely difficult to gather biophysical data from the same leaf over an extended period of time. By developing a predictive, biophysically-based model of leaf optical properties in the visible range (400 nm - 700 nm), such data can be obtained from the non-destructive measurements of leaf spectra.

In the visible range, leaf reflectance and transmittance are influenced primarily by pigments, specifically chlorophylls and carotenoids. Therefore, to develop a biophysically-based model of leaf optical properties in this spectral domain the model parameters should include the light absorption spectra of pigments. Initially the light absorption spectra of chlorophylls and carotenoids were obtained from published literature and combined with their measured concentrations to model leaf spectra. Comparisons showed that the modeled leaf spectra were in poor agreement with the measured leaf spectra. Investigation into the cause of these discrepancies higlighted issues with respect to the use of the measured light absorption spectra of individual pigments in the modeling of leaf optical properties.

Although many researchers have obtained the light absorption spectra of pigments, comparison of published curves shows a lack of agreement between them [55]. The differences among the published light absorption spectra of pigments can often be attributed to the impact of the preparative process on the purity of the pigment and the influence of the solvent used during the measurement process. For example, pigments should be extracted in the dark and measured soon after separation to avoid deterioration [76]. In addition, it has been shown that the same pigment sample measured in different solvents produces light absorption spectra that differ in shape and the wavelength position of their absorption maxima [35]. Furthermore, pigments in a plant leaf (*in vivo*) absorb light differently then those that have been extracted (*in vitro*). This is due to the optical effects associated with the distribution and molecular state of pigments under *in vivo* conditions as well as the leaf tissue itself (Figure 1.1). After extraction, these optical effects disappear, altering the pigments' light absorption spectra. Hence, the measured light absorption spectrum of a given pigment no longer reflects its *in vivo* absorptive properties. Therefore, regardless of which measured light absorption spectrum is used in the simulation of light interaction with leaf tissue, one should take these optical effects into account since they may introduce undue bias into comparisons between modeled and measured foliar spectral data.

(a)

(b)

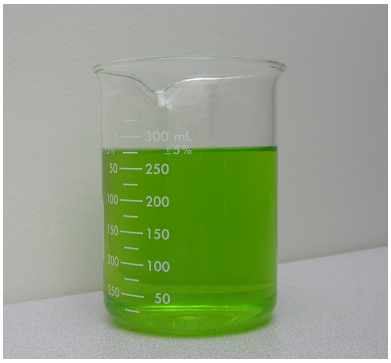

(c)

Figure 1.1: Photographs illustrating chlorophyll occurrence in plant leaves. a) Intact soybean (*Glycine max, Soja hispida*) leaves in their natural state. b) Microscope cross-section of a soybean leaf showing the heterogeneous, *in vivo* distribution of chloroplasts (cellular granules containing chlorophyll) (Photo courtesy of T.F. Chen). c) The homogeneous, *in vitro* distribution of chlorophyll obtained by immersing crushed soybean leaf in acetone.

1.2 Previous Related Work

Leaf optical models have dealt with these issues in a variety of ways. Some focus on optical behavior outside of the visible domain [2, 43, 10, 46]. Others treat the whole leaf tissue as the absorber rather than individual pigments [1, 65, 72, 28]. There are also models that employ the indirectly determined light absorption spectra of pigments. For example, the model described by Yamada and Fujimura [75] expresses absorption as a linear function of pigment content, which uses an unmeasurable constant that must be determined using a data fitting approach. Another example is the PROSPECT model [40] which calculates foliar reflectance and transmittance curves using the specific absorption coefficients of biochemical constituents, including chlorophylls a and b, whose light absorption spectra are combined into a single curve a+b. The specific absorption coefficients of chlorophyll a+b are determined using the PROSPECT model in conjunction with measured data and a data fitting approach, whose description appears in a subsequent publication by Jacquemoud et al. [42]. Similarly, the RAYTRAN model [30] also includes chlorophyll a+b in its formulation.

At present, only three models use the physically measured light absorption spectra of individual pigments to simulate leaf optics in the visible range: LFMOD1 [70, 45], LIBERTY [23] and SLOP [47]. LFMOD1 uses the shifted light absorption spectra of chlorophylls and carotenoids in ethanol and acetone. Testing was performed for a maple leaf using parameters drawn from literature and a comparison of LFMOD1 results against measured reflectance data showed poor quantitative

agreement in the visible range [70]. LIBERTY, an optical model designed for pine needles, uses the shifted light absorption spectra of extracted leaf pigments in acetone. Biophysical and spectral measurements were used to parameterize and validate LIBERTY, which showed inconsistencies with reflectance values in the 400 nm to 700 nm range for both fresh and dried pine needles [23]. SLOP, like LFMOD1, simulates absorption by chlorophylls and carotenoids. To characterize absorption by chlorophylls, Maier et al. [47] measured the light absorption spectra of chlorophyll a and chlorophyll b in dimethyl sulfoxide (DMSO), and then modified the resulting curves to reflect the influence of *in vivo* conditions. In contrast, absorption by carotenoids was determined by the unadjusted light absorption spectra of extracted β-carotene. Using test parameters derived from biophysical measurements, SLOP showed good agreement with the measured spectral data [47].

1.3 Thesis Contribution

In this thesis, we examine the underlying factors involved in the propagation of visible light in plant tissue under *in vivo* conditions, and how the use of *in vitro* data can affect models simulating these phenomena. Furthermore, we investigate the use of photoacoustic absorption spectroscopy [57] to obtain the light absorption spectra of pigments. We introduce a simple conversion technique for deriving the specific absorption coefficients of individual pigments from their measured photoacoustic absorption spectra, one that does not alter the measured curves significantly, and demonstrates the use of these spectra in the modeling of leaf optical properties

in the visible range. Comparison between the modeled and measured foliar spectral curves (reflectance and transmittance) indicate that photoacoustic absorption spectroscopy is a competitive alternative to current methods for obtaining the light absorption spectra of pigments. Furthermore, the use of specific absorption coefficients that are independent of the model and based on direct physical measurements not only mitigates the introduction of bias and mathematical inaccuracies in the simulations but also strengthens their predictability.

1.4 Thesis Organization

The remainder of this thesis is organized as follows. The next chapter, *Measurement Issues and Methods* outlines issues and methods related to the measurement of the absorptive properties of individual pigments. Chapter 3, *Converting Photoacoustic Absorption Spectra to Light Absorption Spectra*, discusses several approaches for converting photoacoustic absorption spectra to light absorption spectra. Chapter 4, *Results and Discussion* presents the results of qualitative and quantitative comparisons used to evaluate the light absorption spectra obtained through light absorption spectroscopy, a data fitting approach and photoacoustic absorption spectroscopy. Chapter 5 concludes with a summary and discusses possible directions for future work.

Chapter 2

Measurement Issues and Methods

In this chapter, we discuss issues related to the absorptive properties of pigments and highlight effects that should be considered when using *in vitro* data to model the optical properties of intact leaves. In addition, we describe direct and indirect methods for measuring the absorptive properties of individual leaf pigments.

2.1 Measurement Issues

The primary pigments that affect the reflectance and transmittance of plants in the visible range are chlorophylls and carotenoids [67], of which chlorophyll a, chlorophyll b and β-carotene are the most common forms found in green plants [29, 66]. To measure these pigments, an extract is prepared using a sample of leaf tissue mixed with an organic solvent, such as acetone (see Figure 1.1b), and then individual pigments are separated using a chromatographic procedure [44] before being

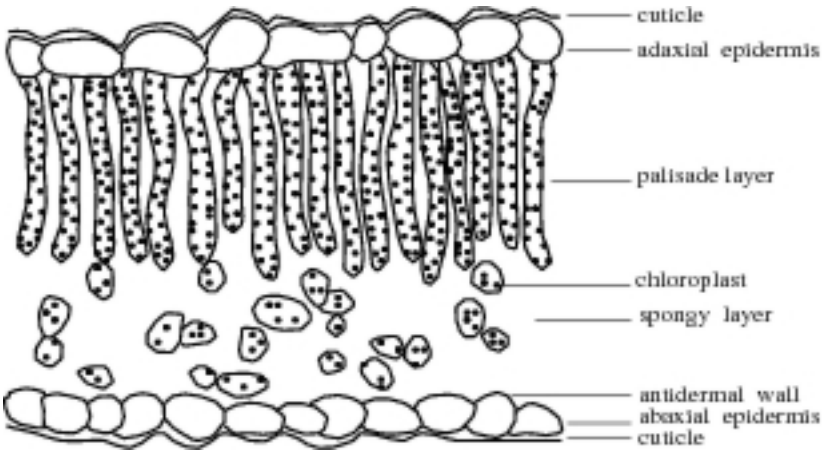

Figure 2.1: Idealized cross-section of leaf tissue [4].

measured. However, due to differences in surrounding environment, distribution and state, the absorption of pigments under *in vitro* conditions differs from that of pigments under *in vivo* conditions. *In vivo* chlorophylls and carotenoids occur as pigment-protein complexes, inhomogeneously distributed throughout leaf tissue which is an intensely scattering medium [56]. These factors affect the passage of light through the leaf and the probability that an incident light ray will be absorbed. Because the extraction process changes the environment, distribution and complexing of pigments, the probability that an incident ray will be absorbed by chlorophylls or carotenoids *in vitro* is not the same as *in vivo*. Consequently, models that use *in vitro* data to characterize pigments must account for these *in vivo* optical effects, otherwise the modeled spectra will not accurately reflect that of an intact leaf.

The cross-section of a typical leaf (as illustrated in Figure 2.1) can be concisely

described as follows. The two outermost layers consist of a waxy cuticle over a layer of close fitting epidermal cells. In between these outer layers is the mesophyll layer, which may be differentiated between cylindrical, densely packed palisade cells and ovoid, more loosely packed spongy cells. The mesophyll cells are where the pigment containing chloroplasts (cellular granules containing chlorophyll) are located.

When an incident light ray passes through the leaf's surface layers into the mesophyll tissue, differences between the refractive indices of intercellular air spaces and cell walls causes the ray to reflect or refract [74]. Multiple internal reflections and refractions of the light ray will lengthen its optical pathlength and increase the probability that it will encounter an absorber. This lengthening of the optical path is referred to as the detour effect, and in comparison to *in vitro* pigments this leads to higher or a steeper rise in *in vivo* absorption values [73, 26]. This is more noticeable in bands of absorption minima since light that was not absorbed under *in vitro* conditions has a greater chance, due to the detour effect, of being absorbed under *in vivo* conditions. In contrast, inhomogeneous distribution of pigments throughout the leaf tissue (Figure 1.1b) can lead to a situation where an incident light ray passes through the leaf without encountering any pigment at all [27]. This is referred to as the sieve effect, and in comparison to *in vitro* pigments it results in lower or a more gradual rise in *in vivo* absorption values. Consequently, the influence of the sieve effect is more noticeable in bands of absorption maxima.

In order to account for changes in the lengthening of the optical path under *in vivo* conditions when using *in vitro* pigment absorption curves, several researchers choose to employ an adjustment parameter known as the factor of intensification

(β) [18], to scale the curves. Values for β have been determined by Ruhle and Wild [60] and McClendon and Fukshansky [49] for several plant species using a statistical mean.

Another issue that must be considered when interpreting *in vitro* light absorption spectra is the occurrence of *in vivo* chlorophylls and carotenoids as pigment-protein complexes [68]. The organic solvent used to prepare leaf extracts destroys pigment-protein bonds and breaks down the complexed form of pigments under *in vitro* conditions. In comparison to *in vivo* pigments, this results in a band shift towards the shorter wavelengths and a flattening of the absorption spectra for *in vitro* pigments [56, 13, 14].

2.2 Measurement Methods

This section describes methods for investigating the absorptive properties of individual leaf pigments: light absorption spectroscopy, a data fitting approach and photoacoustic absorption spectroscopy. Light and photoacoustic absorption spectroscopy obtain direct physical measurements of individual pigments, whereas the data fitting approach uses an indirect method based on whole leaf measurements.

2.2.1 Light Absorption Spectroscopy

The most common method for obtaining the light absorption spectra of pigments is through light absorption spectroscopy. In light absorption spectroscopy, individual

pigments are isolated and purified from prepared leaf extract before being mixed with a solvent. A light spectrometer with an integrating sphere is used to measure how much incident light is reflected and transmitted by the pigment-solvent sample to determine its specific absorption coefficient (s.a.c.). Although many researchers have measured the light absorption spectra of pigments, disagreements between studies exist primarily due to the impact of the extraction and separation process on pigment purity, as well as the influence of the solvent on scattering [55]. From the available literature, we have selected the light absorption spectra for chlorophyll a and chlorophyll b in ethyl ether, and the absorption of β-carotene in hexane (Figure 2.2), to model leaf optical properties in the visible range. These curves have been reconfirmed by other researchers [63, 44] and successfully applied to the quantitative analysis of chlorophylls in leaves [21, 20].

2.2.2 Data Fitting Approach

In contrast to physical measurement methods, many researchers have run simulations in conjunction with data fitting approaches to determine the absorption coefficients of individual constituents from measured data. This process is briefly described as follows. Using the additive nature of absorption [50], leaf tissue is treated as a homogeneous medium whose absorption is calculated by summing the absorption of its biochemical constituents [42, 7, 23, 47]. The absorption of each constituent is calculated by multiplying its concentration by its specific absorption coefficient (s.a.c.). This can be summarized in the following equation:

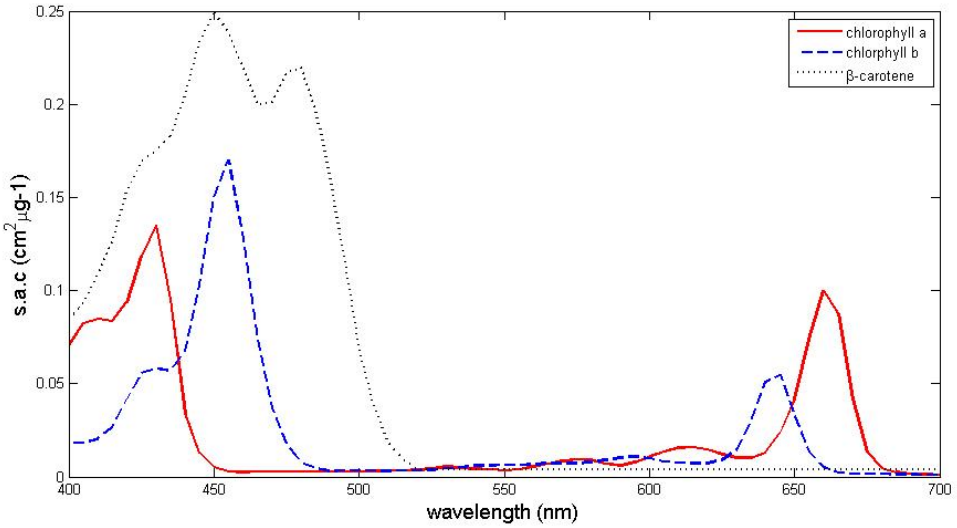

Figure 2.2: Light absorption spectra of chlorophyll a and chlorophyll b in ethyl ether [76] and β-carotene in hexane [77].

$$A(\lambda) = \sum_i a_i(\lambda) c_i \tag{2.1}$$

where $A(\lambda)$ is the leaf absorption at wavelength λ, c_i is the concentration of the ith biochemical constituent, and $a_i(\lambda)$ is the s.a.c. of ith biochemical constituent at wavelength λ.

The model is used to derive leaf absorption from measured reflectance and transmittance spectra. If the measured concentration of the biochemical constituents are known, then applying Equation 2.1 using multiple leaf samples produces a linear system of equations. Using a data fitting approach (e.g., linear least squares [75, 39]), one solves for the unknown $a_i(\lambda)$, i.e., the s.a.c. values of each biochemical

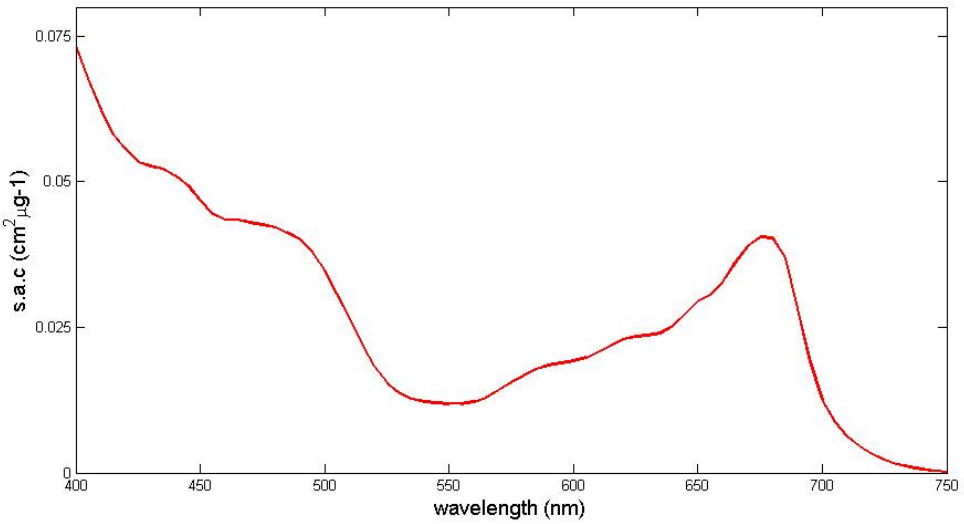

Figure 2.3: Light absorption spectrum of chlorophyll a+b determined using a data fitting method in conjunction with the PROSPECT model [42].

constituent.

Although many candidates for light absorption spectra determined using a data fitting approach exist, we select without loss of generality the curve for chlorophyll a+b provided by Jacquemoud et al. [42] (Figure 2.3) since they have been the subject of several works relating foliar optical properties to biochemical constituents [24, 8].

2.2.3 Photoacoustic Absorption Spectroscopy

Photoacoustic absorption spectroscopy is based on the photothermal effect, introduced by Alexander Graham Bell in 1880. Details on the theoretical foundations

of the photoacoustic effect, experimental setup and applications of photoacoustic absorption spectroscopy in fields such as medicine and biology can be found in texts by Rosencwaig [57, 58]. Briefly, this technique employs a device known as a photoacoustic spectrometer (Figure 2.4), which uses pulsed light to illuminate the material to be measured in an air-tight, gas-filled cell referred to as a photoacoustic or PA cell. The incident light is absorbed which causes molecules of the material to enter into an excited state. These excited molecules de-excite by channeling that absorbed energy into a biophysical process (e.g., photosynthesis), radiation as non-thermal energy (e.g., fluorescence) or radiation as thermal energy or heat emission. When absorbed energy is emitted as heat, it also heats the surrounding gas and causes the pressure inside of the PA cell to increase. The pulsed nature of the incident light causes the pressure to change in a similar manner, generating waves that can be picked up with a detector, such as a microphone (Figure 2.4). The measured strength of the acoustic signal is referenced against the photoacoustic absorption spectrum of carbon black, which is totally light absorbing and totally heat emitting, to determine its relative signal strength. Plotting the relative signal strength generated by the material at different wavelengths of incident light produces a photoacoustic absorption spectra, which qualitatively resembles the light absorption spectra obtained using light absorption spectroscopy (Section 2.2.1).

Photoacoustic absorption spectroscopy has many advantages over other forms of spectroscopy including the ability to obtain the optical and thermal properties of highly-scattering solid and semisolid materials, such as powders, gels, suspensions and tissues. The Rosencwaig-Gersho theory [58] provides a formulation relating

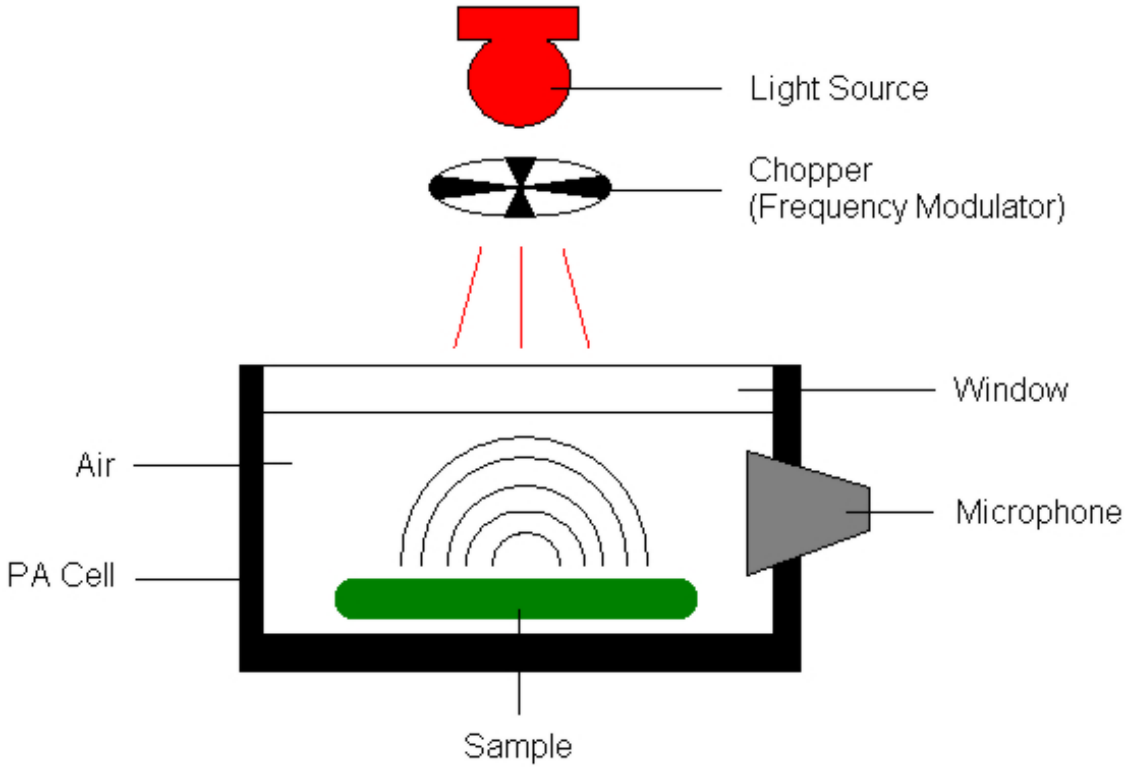

Figure 2.4: A sketch illustrating the main features of a photoacoustic spectrometer.

the depth of the material from which the photoacoustic signal is detected, the thermally active layer, to the rate at which the incident light is pulsed. Due to damping effects, the lower the pulse rate the deeper the thermally active layer is located. Thus this method allows one to conduct non-destructive *in vivo* studies at varying subsurface layers of the sample (depth profile analysis). These advantages make photoacoustic absorption spectroscopy well-suited to the study of plants, particularly photosynthesis research [17, 12, 16, 36, 48]. However, such studies are beyond the scope of this work. Instead our investigations will focus on the

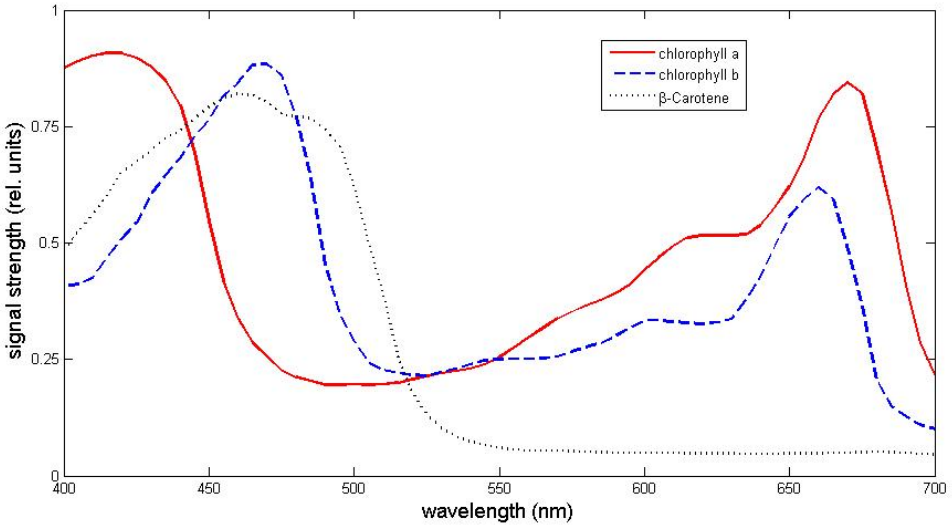

Figure 2.5: Photoacoustic absorption spectra of individual pigments chlorophyll a, chlorophyll b and β-carotene. Relative signal strength is determined by referencing the pigments' measured photoacoustic signal strength against the measured photoacoustic signal of carbon black [52].

photoacoustic absorption spectra of individual pigments isolated from prepared leaf extract i.e., chlorophyll a, chlorophyll b and β-carotene (Figure 2.5). Several approaches for converting the photoacoustic absorption spectrum of a pigment to its corresponding light absorption spectrum for use in the modeling of leaf optical properties will be presented in the next chapter.

Chapter 3

Converting Photoacoustic Absorption Spectra to Light Absorption Spectra

In this chapter, we discuss the underlying physical processes that produce photoacoustic signals and our rationale for treating photoacoustic spectra as light absorption spectra. In addition, we introduce several approaches for converting the photoacoustic signals of individual pigments to specific absorption coefficients for use in the modeling of leaf optical properties.

3.1 Photoacoustic Signals and Light Absorption

Because photoacoustic signals are generated by the non-radiative de-excitation of absorbed energy, photoacoustic absorption spectra closely resemble that of light absorption spectra. However, it is difficult to make direct quantitative comparisons because of other de-excitation processes that can take place, but do not result in the production of heat. For example, in addition to heat emission, pigments can channel absorbed energy into fluorescence emission or photosynthesis [17, 61]. But if either of these processes become blocked or interrupted, a larger percentage of the absorbed energy is emitted as heat, and stronger photoacoustic signals are observed. Buschman and Prehn [15] demonstrated this by comparing the photoacoustic absorption spectra of a healthy leaf with that of one treated with 3-(3,4-dichlorophenyl)-1,1-dimethylurea (DCMU), a chemical that inhibits the electron transport chain used in photosynthesis. The photoacoustic signals observed for the DCMU poisoned leaf were higher than those of the healthy one, as a decrease in photosynthesis led to an increase in heat. Consequently, the photoacoustic absorption spectra comes closer to quantitatively approximating its light absorption spectra.

As described in Section 2.1, under *in vivo* conditions pigments occur as pigment-protein complexes. Two complexes of particular importance for photosynthesis studies are the chlorophyll a protein complex referred to as P700, and the chlorophyll a/b protein complex referred to as P680 [61]. Both P700 and P680 are responsible for performing the photochemical reactions that drive photosynthesis. The role

of other pigments, including chlorophyll b and β-carotene, are to collect and transfer energy to these chlorophyll a complexes. The photoacoustic absorption spectra presented earlier (Figure 2.5) were that of pigments separated from leaf extract using thin layer chromatography (Appendix A). Due to their separation, chlorophyll b and β-carotene are prevented from transferring their captured light energy to P700 and P680, and thus a larger percentage of the absorbed energy is emitted as heat [51]. Furthermore, the organic solvent used to prepare the extract destroys the bonds of the photosynthetically active chlorophyll a complexes. This decrease in photosynthetic ability should also lead to an increase in heat. Our assumption is supported by Veeranjaneyulu and Das [71], who compared the photoacoustic absorption spectra of an intact leaf and its extract in acetone, and observed that the extract exhibited predominately higher photoacoustic signals than that of the leaf. Consequently, we expect that under *in vitro* conditions, separated pigments channel a larger percentage of their absorbed energy into heat emission than any other de-excitation process. This give us reasonable confidence that the photoacoustic absorption spectra of the separated, *in vitro* pigments presented in Figure 2.5 will closely correspond to their light absorption spectra.

3.2 Conversion Guidelines

Several guidelines were adopted to assist in the development of conversion methods for determining s.a.c. values from measured photoacoustic signals.

First, s.a.c. values are equated to corresponding photoacoustic signals at wave-

lengths of weak light absorption. In this study, we are dealing primarily with green plants so wavelengths of weak absorption are those in the green region of the visible spectrum, approximately 500 nm - 560 nm. By focussing on wavelengths of weak light absorption, it is less likely that the critical energy levels necessary to trigger a fluorescent or photosynthetic reaction will be reached. Consequently, this increases the probability that absorbed energy will be channeled into heat emission and the likelihood that a photoacoustic signal will reflect the total amount of absorbed light energy.

Secondly, minimum s.a.c. values are equated to their corresponding photoacoustic signals. As described previously, total absorbed light energy is channeled into photosynthesis, fluorescence and heat emission. Therefore, to minimize the amount of absorbed energy missed by a photoacoustic signal due to photosynthesis and fluorescence we minimize the total absorbed light energy, i.e., focus on minimum s.a.c. values. Again, this increases the likelihood that a photoacoustic signal will come closer to reflecting the total amount of absorbed light energy.

Finally, corresponding s.a.c. values and photoacoustic signals are those found at approximately the same wavelength, as opposed to the exact same wavelength, in order to account for differences between the measurement methods used to obtain each spectra. Pigment s.a.c. values are determined using light absorption spectroscopy and this method requires the pigment to be immersed in solvent for measurement (Section 2.2.1). In contrast, pigment photoacoustic signals are determined using photoacoustic absorption spectroscopy which does not require solvent (Section 2.2.3). As described previously (Section 1.1), solvent causes the absorp-

tion spectra of pigments to shift and so we look at equating values between the two spectra within an narrow wavelength range, about 15 nm (see Section 4.3).

3.3 Intersection Point Approach

A simple approach for converting a photoacoustic absorption spectrum, expressed in relative units, to a light absorption spectrum is to multiply the photoacoustic signals by a selected scaling value. This allows one to obtain the specific absorption spectrum for each pigment that we need to account for in the simulations. Furthermore, if each photoacoustic absorption spectrum is scaled by the same value, the independent nature of the physically measured data is preserved since the shape of each curve is maintained as well as their positions relative to one another. In order to find such a value for all three pigments, we look at the intersection of their curves.

The following formula was used to calculate the scaling value:

$$S_i = \frac{A_{ip}(\lambda)}{P_{ip}(\lambda)}, \tag{3.1}$$

where λ is a wavelength in the green wavelength range, A_{ip} is the specific absorption coefficient at the wavelength corresponding to the intersection of the light absorption spectra and P_{ip} is photoacoustic signal at approximately the same wavelength corresponding to the intersection of the photoacoustic absorption spectra.

To find the intersecting specific absorption coefficient we choose, without loss

of generality (see Section 2.2.1), the light absorption spectra shown in Figure 2.2. From these curves, an intersection point is found at approximately 520 nm with an average specific absorption coefficient of 3781.06 cm^2/g. The photoacoustic spectra of the pigments in Figure 2.5 intersect between 515 nm and 520 nm with an average signal value of 0.213. Applying Equation 3.1 gives a selected scaling value of 17,751.46 cm^2/g.

3.4 Average Approach

Alternatively, a single scaling value can be determined using average values. A new photoacoustic absorption spectra is constructed from the individual photoacoustic absorption curves, by summing the photoacoustic signal for each pigment at each wavelength and dividing by 3:

$$P_{\text{avg}}(\lambda) = \frac{P_a(\lambda) + P_b(\lambda) + P_c(\lambda)}{3}, \tag{3.2}$$

where $P_{avg}(\lambda)$ is the signal value of the new photoacoustic absorption spectra at wavelength λ, $P_a(\lambda)$ is the signal value of chlorophyll a at wavelength λ, $P_b(\lambda)$ is the signal value of chlorophyll b at wavelength λ and $P_c(\lambda)$ is the signal value of β-carotene at wavelength λ.

Similarly, a new light absorption spectra is constructed from the individual light absorption curves by summing the specific absorption coefficient for each pigment

at each wavelength and dividing by 3:

$$A_{\text{avg}}(\lambda) = \frac{A_a(\lambda) + A_b(\lambda) + A_c(\lambda)}{3}, \tag{3.3}$$

where $A_{avg}(\lambda)$ is the specific absorption coefficient of the new light absorption spectra at wavelength λ, $A_a(\lambda)$ is the specific absorption coefficient of chlorophyll a at wavelength λ, $A_b(\lambda)$ is the specific absorption coefficient of chlorophyll b at wavelength λ and $A_c(\lambda)$ is the specific absorption coefficient of β-carotene at wavelength λ.

Using the two new curves P_{avg} and A_{avg}, the scaling value is calculated as follows:

$$S_a = \frac{\min(A_{\text{avg}}(\lambda))}{\min(P_{\text{avg}}(\lambda))}, \tag{3.4}$$

where λ is a wavelength in the green wavelength range, $\min(A_{\text{avg}}(\lambda)$ is the specific absorption coefficient at the wavelength corresponding to the minimum average specific absorption coefficient and $\min(P_{\text{avg}}(\lambda)$ is the minimum average photoacoustic signal at approximately the same wavelength.

Using the light absorption spectra in Figure 2.2 to determine the new light absorption spectrum $A_{\text{avg}}(\lambda)$ this gives a minimum A_{avg} value of 3781.06 cm^2/g at 520 nm. Similarly, the photoacoustic absorption spectra presented in Figure 2.5 are used to generate the new curve $P_{\text{avg}}(\lambda)$, which gives a minimum P_{avg} value of 0.180 at 535 nm. Using Equation 3.4, the calculated scaling value is 21,005.89 cm^2/g.

Table 3.1: Scaling values, calculated using the minimum approach, for converting photoacoustic absorption spectra to light absorption spectra.

Pigment	λ	$A_{\min}(\lambda)$	$P_{\min}(\lambda)$	S_m
chlorophyll *a*	500 nm - 505 nm	0.195	2805.76 cm^2/g	14,388.51 cm^2/g
chlorophyll *b*	510 nm - 525 nm	0.214	3194.80 cm^2/g	14,928.97 cm^2/g
β-carotene	545 nm - 560 nm	0.054	4125.01 cm^2/g	76,389.07 cm^2/g

3.5 Minimum Approach

In the intersection approach (see Section 3.3), a single scaling value was calculated for the three photoacoustic absorption spectra in order to preserve the position of the curves relative to one another. In the minimum approach this criteria is relaxed and a separate scaling value is determined for each photoacoustic absorption spectrum. Thus, the scaling value for a pigments' photoacoustic absorption spectrum, denoted by S_m, is calculated as follows:

$$S_m = \frac{A_{\min}(\lambda)}{P_{\min}(\lambda)}, \tag{3.5}$$

where λ is a wavelength in the green wavelength range, A_{min} is the specific absorption coefficient at the wavelength corresponding to the minimum specific absorption coefficient and P_{min} is the minimum photoacoustic signal at approximately the same wavelength.

Table 3.1 presents the scaling values calculated for each pigment using the light absorption and photoacoustic absorption spectra shown in Figure 2.2 and 2.5.

Chapter 4

Results and Discussion

This chapter presents experimental results used to assess the impact of different light absorption spectra on the modeling of leaf optical properties in the visible range. Both quantitative and qualitative comparisons of modeled reflectance and transmittance with actual measured data are used to determine how closely light absorption spectra obtained through the methods discussed in Chapter 2 (absorption spectroscopy, a data fitting approach and photoacoustic absorption spectroscopy) reflect the absorptive properties of *in vivo* pigments. These comparisons highlight the importance of *in vivo* optical effects by modeling with raw and adjusted light absorption spectra. Furthermore, they demonstrate the effectiveness of using the converted photoacoustic absorption spectra presented in Chapter 3 in the simulation of foliar optics.

4.1 Experimental Setup

This section describes the biophysically-based model of leaf optical properties, measured data and light absorption spectra used in our computational experiments.

4.1.1 Modeling Leaf Optical Properties

To model the leaf optical properties of plant leaves, we use the ABM-B model [7, 3]. ABM-B uses Monte-Carlo methods to simulate the passage of light photons through plant tissue. Probability distributions calculated from parameters relating to leaf physiology and biochemical constituents are used to randomly determine whether a photon is absorbed, reflected or refracted. For a detailed description of these models, we refer the interested reader to recent publications by Baranoski [7] and Baranoski and Eng [3]. The ABM-B model was selected due to the ease with which the light absorption spectra of individual pigments could be incorporated into the simulation. Furthermore, its predictability has been evaluated against measured data [7].

The ABM-B model was originally employed to simulate the interaction of infrared radiation (750 nm - 2500 nm) with plant leaves. In order to allow its use to simulate the interaction of visible light (400 nm - 700 nm) with foliar tissue, its parameter space required several modifications. Absorption in the visible range is dominated by pigments. Consequently, absorption by other leaf constituents is considered negligible and the specific absorption coefficients of protein and cellu-

lose+lignin were set to zero. The light absorption spectrum of water was obtained from data measurements performed by Pope and Fry [54]. In addition, its refractive index was set to an average value of 1.33 since it does not vary significantly in the visible range [34]. Finally, with the incorporation of pigments in the modeling of leaf optical properties, the calculation of the effective absorption coefficient was modified to include the specific absorption coefficient and concentration of chlorophyll *a*, chlorophyll *b* and carotenoids.

4.1.2 Measured Biophysical and Spectral Data

The measured biophysical data for testing and spectral data (reflectance and transmittance) for evaluating the modeled leaf spectra was obtained from the Leaf Optical Properties Experiment (LOPEX) database [38]. The LOPEX database is the result of a series of experiments carried out in 1993 where the biophysical and spectral characteristics of over 50 different plant species were measured and recorded. We selected, without loss of generality, soybean (*Glycine max, Soja hispida*) because of its standard foliar characteristics and the large variety of experimental data available for comparison [11, 33, 74]. For soybean reflectance and transmittance we used LOPEX spectral files 0219 and 0220. A virtual spectrophotometer was used to generate the modeled spectra for comparison [6].

Table 4.1 presents the LOPEX biophysical data used to determine the concentration of constituents. The steps used to calculate the concentration of protein and cellulose+lignin are described by Baranoski [7]. Pigment concentration was

Table 4.1: Measured (LOPEX) biophysical data used to compute the soybean modeled spectral signatures.

Biophysical measurement	Value
Area (cm^2)	4.10
Thickness (cm)	0.0166
Fresh weight (g)	0.0494
Dry weight (g)	0.0119
Protein concentration (%)	31.64
Cellulose concentration (%)	16.83
Lignin concentration (%)	2.90
Fresh chlorophyll a content (mg/g)	2.74
Fresh chlorophyll b content (mg/g)	0.80
Fresh carotenoid content (mg/g)	0.78

calculated by multiplying the fresh weight content of each pigment by the fresh weight of the leaf, and dividing that result by the mesophyll volume. The mesophyll volume was chosen, as opposed to leaf volume, since pigments are located in chloroplasts, almost all of which are found in the mesophyll tissue [9]. The mesophyll volume was determined by multiplying leaf area by mesophyll thickness, suggested by Baranoski [7] to be 50% of the total leaf thickness.

In addition to the concentration of constituents, aspect ratios used to characterize the shape of cells in the cuticular, epidermal and mesophyll layers of the leaf were specified [7]. Table 4.2 presents a summary of the parameter values used to model the soybean specimens used in our experiments.

Table 4.2: Biophysical parameters used to compute the soybean modeled spectral signatures.

Symbol	Biophysical parameter	Value
t_m	Thickness of mesophyll (cm)	0.00830
C_p	Concentration of protein (g/cm^3)	0.0801
C_l	Concentration of cellulose+lignin (g/cm^3)	0.0499
C_a	Concentration of chlorophyll a (g/cm^3)	0.003978
C_b	Concentration of chlorophyll b (g/cm^3)	0.001161
C_c	Concentration of carotenoids (g/cm^3)	0.001132
δ_c	Aspect ratio of cuticle	5.0
δ_e	Aspect ratio of epidermis	5.0
δ_p	Aspect ratio of palisade mesophyll	1.0
δ_s	Aspect ratio of spongy mesophyll	5.0

4.1.3 Light Absorption Spectra

Modeled spectral curves for soybean were generated using light absorption spectra obtained directly through light absorption spectroscopy (AS), indirectly using a data fitting approach (DFA) and converted from photoacoustic absorption spectra (PAS) (Figure 2.2 - 2.5). The light absorption spectra corresponding to each of these methods are referred to as the AS, DFA and PAS light absorption spectra, respectively. Similarly, the modeled spectral curves corresponding to each of these light absorption spectra are referred to as the AS, DFA and PAS modeled spectral curves, respectively.

The AS and PAS light absorption spectra correspond to individual pigments while the DFA light absorption spectrum corresponds to the combined absorption of chlorophylls a and b. Consequently, when using this curve as input to the leaf optical model, it was treated as the light absorption spectrum of chlorophyll a. The concentration of chlorophyll a was set to include the concentration of chlorophyll b, while the concentration of both chlorophyll b and β-carotene were set to zero.

The PAS light absorption spectra were obtained by converting photoacoustic absorption spectra to light absorption spectra using the intersection point approach (see Section 3.3). The intersection point approach was selected instead of the average or minimum approach (see Sections 3.4 and 3.5) because the modeled leaf spectra using this method comes closest to approximating the measured leaf spectra. This aspect is demonstrated by comparisons presented in Appendix B.

4.2 Curves Using Raw Light Absorption Spectra

The graphs presented in Figures 4.1 and 4.2 show good quantitative and qualitative agreement using the DFA light absorption spectra. In contrast, modeled results using the PAS light absorption spectra are qualitatively similar but both reflectance and transmittance values are higher than the measured data. The AS modeled spectral curves show the greatest difference, both qualitatively and quantitatively, when compared with the LOPEX curves. From 400 nm to 500 nm, there is close quantitative agreement before the curve sharply rises. Between 500 nm and 640 nm, the modeled values are higher than the measured values, and three minor minima occur at 530 nm, 575 nm and 615 nm. In Figure 4.2, the curve also exhibits a distinct minimum at 660 nm, that drops transmittance values below the measured values.

To assist in the evaluation of the quantitative differences between the modeled and measured spectra, the corresponding root mean square error (RMSE) values have been computed (Table 4.3). The RMSE values for the spectra generated using the DFA light absorption spectra are less than 0.03, which according to Jacquemoud et al. [42] indicates good spectral reconstruction for both reflectance and transmittance. The RMSE values for the AS and PAS modeled spectra are quite high, between 0.0846 and 0.1423, highlighting the poor quantitative agreement with the actual measured data as observed in Figure 4.2.

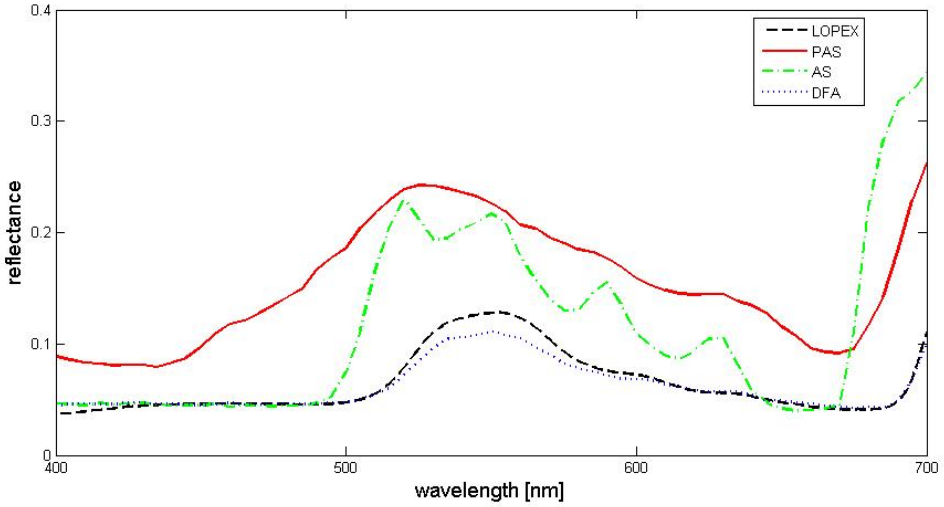

Figure 4.1: Comparison between measured (LOPEX) and modeled (ABM-B) *reflectance* curves of soybean leaf (*Glycine max, Soja hispida*). Modeled curves were generated using pigment light absorption spectra obtained through light absorption spectroscopy (AS), a data fitting approach (DFA) and photoacoustic absorption spectroscopy (PAS).

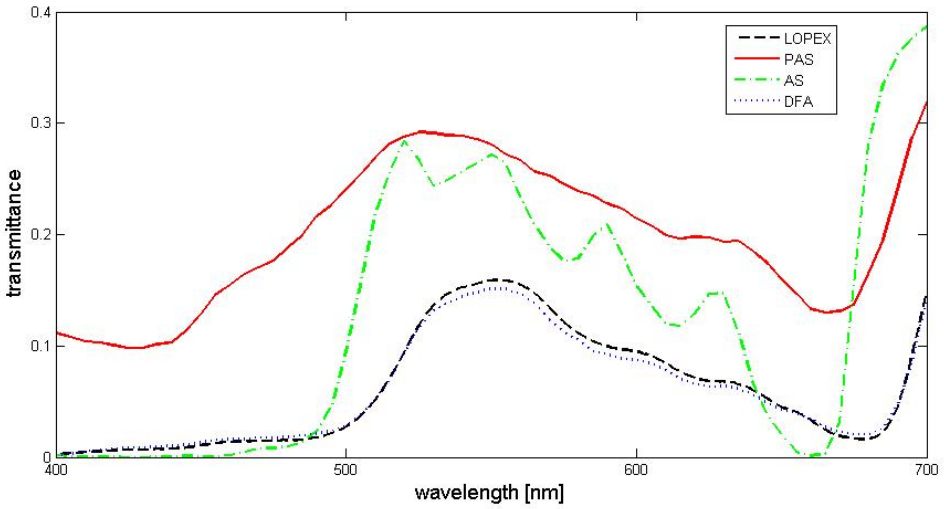

Figure 4.2: Comparison between measured (LOPEX) and modeled (ABM-B) *transmittance* curves of soybean leaf (*Glycine max, Soja hispida*). Modeled curves were generated using pigment light absorption spectra obtained through light absorption spectroscopy (AS), a data fitting approach (DFA) and photoacoustic absorption spectroscopy (PAS).

Table 4.3: Computed root mean square error (RMSE) values for the modeled soybean spectra using raw light absorption spectra.

	AS	DFA	PAS
reflectance	0.0846	0.0074	0.0961
transmittance	0.1081	0.0049	0.1419

4.3 Curves Using Adjusted Light Absorption Spectra

A second set of modeled curves were generated using adjusted AS and PAS light absorption spectra. Adjustments were made to account for optical effects associated with *in vivo* pigments. No adjustments were necessary for the DFA light absorption spectrum since it was obtained using a process that computes absorption values from whole leaf values. Hence, it implicitly account for *in vivo* effects (see Section 2.1).

The first adjustment involved correcting for the detour effect. As previously discussed in Measurement Issues (see Section 2.1), the detour effect is caused by leaf tissue, which is a highly scattering medium. The optical pathlength of incident rays is lengthened and this increases the probability of absorption under *in vivo* conditions. Based on factors of intensification (β) computed for different plant species with respect to different pigment concentrations [60], we have selected the β values presented in Table 4.4 to scale the light absorption spectra (AS and PAS) employed in our second set of experiments. Details of the procedure used to select these values are provided in Appendix C.

The second adjustment involved a shift of the pigment light absorption spectra towards the red in order to account for *in vivo* pigment-protein complexes. The spectral shift of chlorophyll a has been estimated by several researchers to be 15 nm [19, 55]. Although it has been established that chlorophyll b and carotenoids

Table 4.4: Factors of intensification selected for the pigments chlorophyll a (β_a), chlorophyll b (β_b) and β-carotene (β_c) based on published values [60].

Factor of Intensification	Value
β_a	2.0
β_b	4.1
β_c	4.1

undergo a similar *in vivo* to *in vitro* spectral shift, it has been more difficult to determine since the more strongly absorbing chlorophyll a masks their *in vivo* absorption bands [55]. Therefore, to avoid any undue bias, a uniform shift of 15 nm has been applied to all pigment light absorption spectra.

Figures 4.3 and 4.4 show an improved quantitative agreement obtained using the adjusted PAS light absorption spectra. Both the modeled transmittance and reflectance values were lowered and more closely resemble the measured values. The AS modeled spectra also show improvements, however they are not as significant. Although the reflectance and transmittance values were lowered, they were generally below the measured values. This difference is particularly noticeable in Figure 4.4 between the wavelength ranges 400 nm to 510 nm, and 660 nm to 690 nm, where transmittance values are close to zero. Furthermore, the AS modeled spectra using both the raw and adjusted light absorption spectra display the same minor minima. In the AS modeled spectra using the adjusted light absorption spectra these minor minima occur at approximately 545 nm, 690 nm and 630 nm, which corresponds to our shift of the pigment absorption spectra by 15 nm.

Table 4.5: Computed root mean square error (RMSE) values for the modeled soybean spectra using adjusted light absorption spectra.

	AS	DFA	PAS
reflectance	0.0182	0.0074	0.0102
transmittance	0.0315	0.0049	0.0172

Table 4.5 presents the RMSE values for the curves shown in Figure 4.3 and 4.4. With the exception of the transmittance curve generated using the AS light absorption spectra, values are less 0.03, which indicates good spectral reconstruction [42]. The RMSE values are smaller than those computed for the raw light absorption spectra (Table 4.3), demonstrating improved quantitative agreement using the adjusted light absorption spectra.

4.4 Discussion

Based on our experiments, the DFA and adjusted PAS light absorption spectra produced the closest approximations with respect to the measured (LOPEX) spectral curves. We remark, however, that the use of PAS light absorption spectra allows the incorporation of separate data for individual pigments in the simulations. In addition, the PAS light absorption spectra are determined through direct physical measurement, i.e., independent of any particular model or process. These aspects illustrate the advantages of using PAS light absorption spectra in the modeling of foliar optical properties.

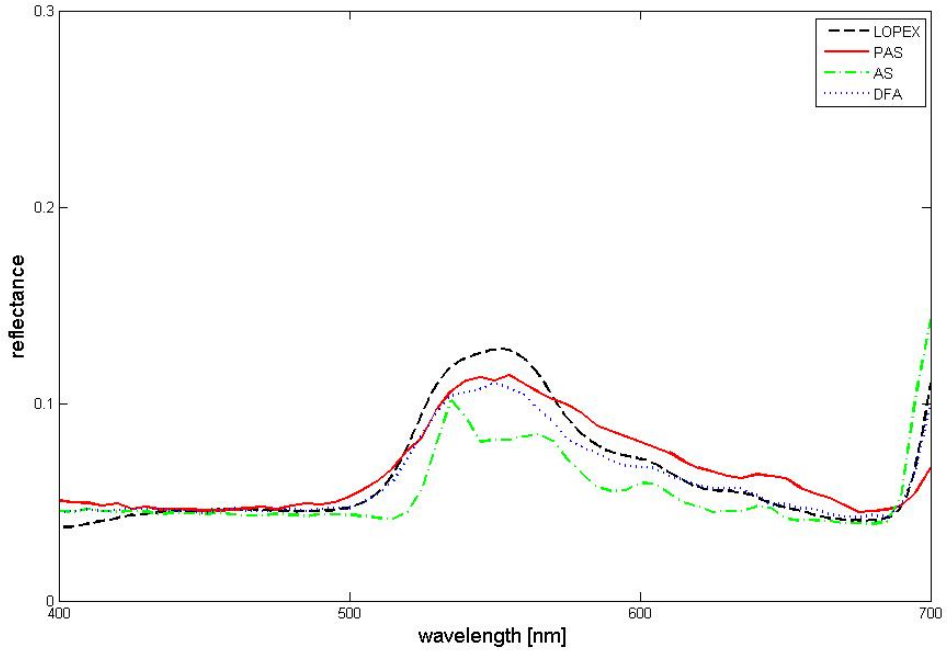

Figure 4.3: Comparison between measured (LOPEX) and modeled (ABM-B) *reflectance* curves of soybean leaf (*Glycine max, Soja hispida*). Modeled curves were generated using pigment light absorption spectra obtained through light absorption spectroscopy (AS), a data fitting approach (DFA) and photoacoustic absorption spectroscopy (PAS). The AS and PAS light absorption spectra were multiplied by factors of intensification β (Table 4.4) and shifted 15 nm to account for *in vivo* optical effects.

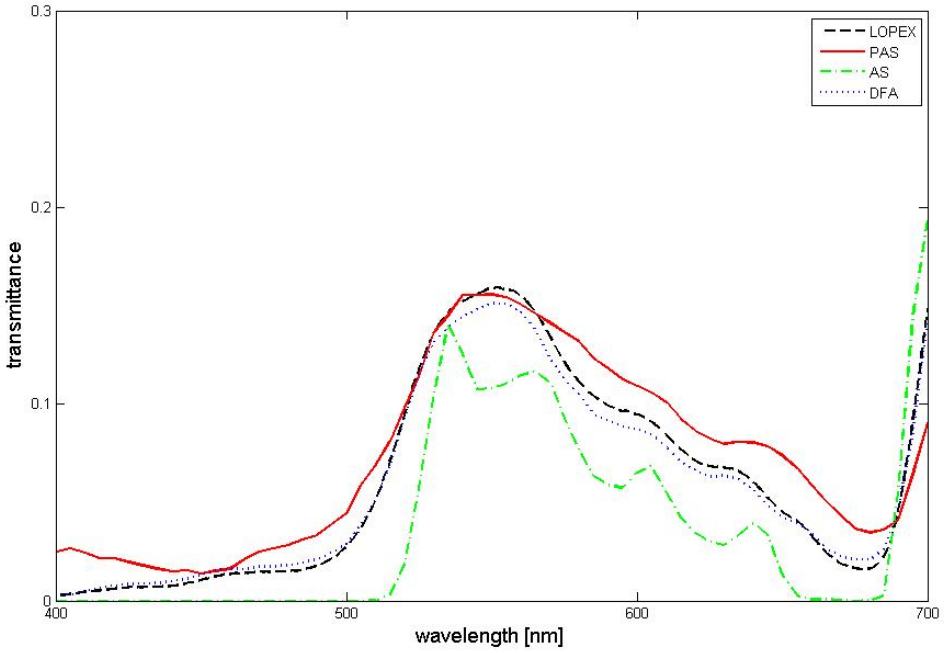

Figure 4.4: Comparison between measured (LOPEX) and modeled (ABM-B) *transmittance* curves of soybean leaf (*Glycine max, Soja hispida*). Modeled curves were generated using pigment light absorption spectra obtained through light absorption spectroscopy (AS), a data fitting approach (DFA) and photoacoustic absorption spectroscopy (PAS). The AS and PAS light absorption spectra were multiplied by factors of intensification β (Table 4.4) and shifted 15 nm to account for *in vivo* optical effects.

An open issue related to the PAS light absorption spectra is its reliance on the selected conversion method and in particular, the selected scaling value used to convert the photoacoustic signal values to specific absorption coefficients. Although we have adopted a simple approach, one that avoids making any modifications to the shape or position of the original photoacoustic absorption spectra, other alternatives may exist. This is a potential avenue for future work. However, regardless of the scaling value applied, it is evident that qualitatively the PAS light absorption spectra more closely reflects the absorption of pigments, especially when compared with results produced by the AS light absorption spectra.

The AS modeled spectra exhibited three minor minima at 530 nm, 575 nm and 615 nm. Similarly, the adjusted AS modeled spectra exhibited a shift in the minima, which is consistent with the 15 nm shift of the pigment spectra. Further investigation shows that the wavelength positions of these minima correspond to the wavelength positions of minima in the chlorophyll *a* light absorption curve (Figure 2.2). Comparison of the original light absorption spectra and the original photacoustic absorption spectra of chlorophyll *a* (Figure 2.2 and 2.5) shows that in the wavelength range from 550 nm to 650 nm, the light absorption spectra fluctuates whereas the photoacoustic absorption spectra is smooth. The smoothness of the photoacoustic curve in this region can be attributed to the increased sensitivity of photoacoustic absorption spectroscopy to low concentrations of pigments [32, 59, 52]. Furthermore, as discussed previously in Section 2.2.1, light absorption spectroscopy requires pigment to be mixed with a solvent before being measured with an integrating sphere. Comprehensive studies of the influence of solvent on

light absorption spectra has been carried out by Seely and Jensen [62] and Harris and Zscheile [35]. In contrast, photoacoustic absorption spectroscopy does not require the pigment to be immersed in solvent during measurement (Appendix A). Thus its sensitivity and the elimination of solvent in the measurement process, give photoacoustic absorption spectroscopy an advantage over light absorption spectroscopy when measuring the absorptive properties of individual pigments.

Chapter 5

Conclusion

The biophysically-based modeling of leaf optical properties in the visible range using individual pigments has clearly proven to be a difficult task. As outlined previously, many models focus on wavelengths outside of this spectral domain or treat absorption at the tissue level, which avoids having to address absorption by individual pigments.

Typical methods for determining the absorptive properties of pigments are direct measurement using light absorption spectroscopy, or by applying a data fitting approach to measured spectral data. In this thesis, we introduced a third alternative, one that uses photoacoustic absorption spectra to determine the specific absorption coefficients of the leaf pigments chlorophyll a, chlorophyll b and β-carotene. In order to avoid significant modifications to the physically-measured curve, a simple scaling procedure to convert photoacoustic signals to their corresponding specific

absorption coefficients was proposed. This conversion method was evaluated by performing a comparison of the modeled results using the different light absorption spectra. Our results showed that, once *in vivo* optical effects had been taken into account, the converted photoacoustic absorption spectra produced results that were in good agreement with measured spectral curves.

To address the problem of obtaining accurate *in vivo* light absorption spectra, many studies have adopted a data fitting approach. To the best of our knowledge, our study is the first work to introduce a measurement method, namely photoacoustic spectroscopy, as a potential solution. The demonstrated applicability of photoacoustic absorption spectra in the modeling of leaf optical properties using individual pigments is strong evidence that photoacoustic absorption spectroscopy is a competitive alternative to current methods. Furthermore, we have highlighted the importance of considering *in vivo* optical effects when using *in vitro* light absorption spectra to model foliar optics. Our computational experiments showed that although the process used by the data fitting approach to obtain the light absorption spectra of pigments implicitly includes the influence of the detour effect and pigment-protein complexes, the light absorption spectra obtained from light and photoacoustic absorption spectroscopy do not and should be adjusted accordingly.

While photoacoustic absorption spectroscopy has primarily been used to investigate the properties of foliar tissue, we hope that this work motivates further research into the application of this method for the study of individual biochemical constituents. Researching alternative approaches for converting the photoacoustic

signals of biochemical constituents to specific absorption coefficients and expanding the scope of our observations would help to improve our understanding and use of photoacoustic absorption spectra. In addition, we hope to address the intial motivation of our research: using measured spectral curves to investigate the physiological and biochemical changes a leaf undergoes due to plant senesence or aging. Finally, although this thesis has focused on the use of photoacoustic absorption spectra to model the optical properties of plant leaves, such spectra may also be suitable for modeling the optical properties of other biological tissues with light absorbing constituents. These are issues that we hope to investigate in future work.

Bibliography

[1] Allen, W., H. Gausman, A. Richardson, and J. Thomas (1969) Interaction of isotropic light with a compact leaf. *Journal of the Optical Society of America.* 59(10):1376–1379.

[2] Allen, W. and A. Richardson (1973) Willstater-Stoll theory of leaf reflectance evaluated by ray tracing. *Applied Optics.* 12(10):2448–2453.

[3] Baranoski, G. V. and D. Eng (2006) An investigation on sieve and detour effects affecting the interaction of infrared radiation with plant leaves. Technical Report Technical Report CS-2006-02, School of Computer Science, University of Waterloo, Canada.

[4] Baranoski, G. V. and J. G. Rokne (1997) An algorithmic reflectance and transmittance model for plant tissue. *Computer Graphics Forum (Proc. of Eurographics '97).* 16(3):141–150.

[5] Baranoski, G. V. and J. G. Rokne (2004) Light Interaction With Plants: A Computer Graphics Perspective. Horwood Publishing, Chichester, England.

[6] Baranoski, G. V., J. G. Rokne, and G. Xu (2001) Virtual spectrophotometric measurements for biologically and physically-based rendering. *The Visual Computer.* 17(8):506–518.

[7] Baranoski, G. V. G. (2006) Modeling the interaction of infrared radiation (750 to 2500nm) with bifacial and unifacial plant leaves. *Remote Sensing of Environment.* 100(3):335–357.

[8] Baret, F. and T. Fourty (1997) Estimation of leaf water content and specific leaf weight from reflectance and transmittance measurements. *Agronomy.* 17:455–464.

[9] Björn, L. O. (1992) Interception of light by leaves. *In* Crop Photosynthesis: Spatial and Temporal Determinants. N. R. Baker and H. Thomas, Editors. Elsevier Science, Amsterdam. 253–276.

[10] Brakke, T. W. and J. A. Smith (1987) A ray tracing model for leaf bidirectional scattering studies. *IGARSS '87: Proc. of the International Geosciences and Remote Sensing Symposium.* 643–648.

[11] Breece, H. T. and R. A. Holmes (1971) Bidirectional scattering characteristics of healthy green soybean and corn leaves *in vivo*. *Applied Optics.* 10(1):119–127.

[12] Buschmann, C. (1989) Photoacoustic measurements: Applications in plant science. *Philosophical Transactions of the Royal Society of London, Series B.* 323(1216):423–434.

[13] Buschmann, C. and N. Eckehard (1991) Reflection spectra of terrestrial vegetation as influenced by pigment-protein complexes and the internal optics of leaf tissue. *IGARSS '91: Proc. of the International Geoscience and Remote Sensing Symposium.* 1909–1912.

[14] Buschmann, C. and E. Nagel (1993) In vivo spectroscopy and internal optics of leaves as basis for remote sensing of vegetation. *International Journal of Remote Sensing.* 14(4):711–722.

[15] Buschmann, C. and H. Prehn (1981) In vivo studies of radiative and non-radiative de-excitation processes of pigments in raphanus seedlings by photoacoustic spectroscopy. *Photobiochemistry and Photobiophysics.* 2:209–215.

[16] Buschmann, C. and H. Prehn (1990) Photoacoustic spectroscopy - photoacoustic and photothermal effects. *In* Modern Methods of Plant Analysis, Vol. II. H. F. Linskens and J. F. Jackson, Editors. Springer-Verlag, Berlin. 148–180.

[17] Buschmann, C., H. Prehn, and H. Lichtenthaler (1984) Photoacoustic spectroscopy (PAS) and its application in photosynthesis research. *Photosynthesis Research.* 5:29–46.

[18] Butler, W. H. (1964) Absorption spectroscopy in vivo: Theory and applications. *Annual Review of Plant Physiology.* 15:451–460.

[19] Charney, E. and F. S. Brackett (1961) The spectral dependence of scattering from a spherical alga and its implications for the state of organization of the light-accepting pigments. *Archives of Biochemistry and Biophysics.* 92(1):1–12.

[20] Comar, C. L., E. J. Benne, and E. K. Buteyn (1943) Calibration of photoelectric colorimeter for determination of chlorophyll - relation between spectra of standards and accuracy of analytical results. *Industrial & Engineering Chemistry Analytical Edition.* 15(8):524–526.

[21] Comar, C. L. and F. P. Zscheile (1942) Analysis of plan extracts for chlorophylls a and b by a photoelectric spectrophotometric method. *Plant Physiology.* 17:198–209.

[22] Curran, P. J. (2001) Imaging spectrometry for ecological applications. *International Journal of Applied Earth Observation and Geoinformation .* 3(4):305–312.

[23] Dawson, T., P. Curran, and S. Plummer (1998) LIBERTY: Modeling the effects of leaf biochemical concentration on reflectance spectra. *Remote Sensing of Environment.* 65:50–60.

[24] Fourty, T., F. Baret, S. Jacquemoud, G. Schmuck, and J. Verdebout (1996) Leaf optical properties with explicit description of its biochemical composition: Direct and inverse problems. *Remote Sensing of Environment.* 56:104–117.

[25] Fried, B. and J. Sherma (1999) Thin-layer Chromatography (Chromatographic Science, Vol. 81), 4th Ed. Marcel-Dekker, Inc., New York. 9–11.

[26] Fukshansky, L. (1981) Optical properties of plants. *In* Plant and the Daylight Spectrum. H. Smith, Editor. Academic Press, London. 21–40.

[27] Fukshansky, L. (1991) Photon transport in leaf tissue: Applications in plant physiology. *In* Photon-Vegetation Interactions. R. Myneni and J. Ross, Editors. Springer-Verlag, Berlin. 253–302.

[28] Ganapol, B., L. Johnson, P. Hammer, C. Hlavka, and D. Peterson (1998) LEAFMOD: A new within-leaf radiative transfer model. *Remote Sensing of Environment.* 63:182–193.

[29] Gates, D. M., H. J. Keegan, J. C. Schleter, and V. R. Weidner (1965) Spectral properties of plants. *Applied Optics.* 41(1):11–20.

[30] Govaerts, Y., S. Jacquemoud, M. Verstraete, and S. Ustin (1996) Three-dimensional radiation transfer modeling in a dycotyledon leaf. *Applied Optics.* 35(33):6586–6598.

[31] Greenberg, D., J. Arvo, E. Lafortune, K. Torrance, J. Ferwerda, B. Walter, B. Trumbore, P. Shirley, S. Pattanaik, and S. Foo (1997) A framework for realistic image synthesis. *SIGGRAPH '97: Proc. of the 24th annual conference on computer graphics and interactive techniques.* 477–494.

[32] Guiwen, Z., C. Hua, L. Siquan, and S. Qingde (1990) Identification of chlorophylls and carotenoids by photoacoustic spectroscopy. *In* Photoacoustic and Photothermal Phenomena II. J. Murphy, J. M. Spicer, L. Aamodt, and B. Royce, Editors. Springer, Berlin. 442–444.

[33] Gupta, R. K. and J. T. Wooley (1971) Spectral properties of soybean leaves. *Agronomy Journal.* 63:123–126.

[34] Hale, G. M. and M. R. Querry (1973) Optical constants of water in the 20-nm to 200-um wavelength region. *Applied Optics.* 12(3):555–563.

[35] Harris, D. G. and F. P. Zscheile (1943) Effects of solvent upon absorption spectra of chlorophylls a and b; their ultraviolet absorption spectra in ether solution. *Botanical Gazette.* 104:515–527.

[36] Herbert, S. K., T. Han, and T. C. Vogelmann (2000) New applications of photoacoustics to the study of photosynthesis. *Photosynthesis Research.* 66:13–31.

[37] Horler, D. N. and J. Barber (1981) Principles of remote sensing of plants. *In* Plant and the Daylight Spectrum. H. Smith, Editor. Academic Press, London. 44–63.

[38] Hosgood, B., S. Jacquemoud, G. Andreoli, J. Verdebout, G. Pedrini, and G. Schmuck. (1995) Leaf optical properties experiment 93 (LOPEX93). Technical Report EUR-16095-EN, Joint Research Center, European Commission, Institute for Remote Sensing Applications, Ispara, Italy.

[39] Jacquemoud, S. (2004) New calibration of PROSPECT. Technical report, Université Paris 7 - Institut de Physique du Globe de Paris, Paris, France.

[40] Jacquemoud, S. and F. Baret (1990) PROSPECT: A model of leaf optical properties spectra. *Remote Sensing of Environment.* 34(2):75–92.

[41] Jacquemoud, S. and S. Ustin (2001) Leaf optical properties: State of the art. *Proc. of the 8th International Symposium of Physical Measurements and Signatures in Remote Sensing.* 223–332.

[42] Jacquemoud, S., S. L. Ustin, J. Verdebout, G. Schmuck, G. Andreoli, and B. Hosgood (1996) Estimating leaf biochemistry using PROSPECT leaf optical properties model. *Remote Sensing of Environment.* 56:194–202.

[43] Kumar, R. and L. Silva (1973) Light ray tracing through the leaf cross section. *Applied Optics.* 12(12):2950–2954.

[44] Lichtenthaler, H. K. (1987) Pigments of photosynthetic biomembranes. *In* Methods of Enzymology: Plant Cell Membranes, Vol. 148. L. Packer and R. Douce, Editors. Academic Press, New York. 350–382.

[45] Ludeker, W. and K. P. Gunther (1990) Leaf reflectance: A stochastic model for analysing the blue shift. *Proc. of the Symposium on Global and Environmental Monitoring.* 475–480.

[46] Ma, Q., A. Nishimura, P. Phu, and Y. Kuga (1990) Transmission, reflection and depolarization of an optical wave for a single leaf. *IEEE Transaction on Geoscience and Remote Sensing.* 28(5):865–872.

[47] Maier, S., W. Ludeker, and K. Gunther (1999) SLOP: A revised version of the stochastic model for leaf optical properties. *Remote Sensing of Environment.* 682:273–280.

[48] Malkin, S. and O. Canaani (1994) The use and characteristics of the photoacoustic method in the study of photosynthesis. *Annual Review of Plant Physiology and Plant Molecular Biology.* 45:493–526.

[49] McClendon, J. H. and L. Fukshansky (1990) On the interaction of absorption spectra of leaves - ii. the non-absorbed ray of the sieve effect and the mean optical pathlength in the remainder of the leaf. *Photochemistry and Photobiology.* 51(2):211–216.

[50] Meyer-Arendt, J. R. (1984) Introduction to Classical and Modern Optics, 2nd Ed. Prentice-Hall, Englewood Cliffs, N.J. 481–491.

[51] Nagel, E. M., C. Buschmann, and H. K. Lichtenthaler (1987) Photoacoustic spectra of needles as an indicator of the activity of the photosynthetic apparatus of healthy and damaged conifers. *Physiologia Plantarum.* 70:427–437.

[52] Nagel, E. M., H. K. Lichtenthaler, L. Koschanyl, and P. A. Biacs (1989) Photoacoustic spectra of chlorophylls and carotenoids in fruits and in plant oils. *In* Biological Role of Plant Lipids. P. A. Biacs, K. Guiz, and T. Kremmer, Editors. Plenum Publishing, New York and London. 271–273.

[53] Nagler, P. L., C. S. Daughtry, and S. N. Goward (2000) Plant litter and soil reflectance. *Remote Sensing of Environment.* 71(2):207–215.

[54] Pope, R. M. and E. S. Fry (1997) Absorption spectrum (380 -700 nm) of pure water. ii. integrating cavity measurements. *Applied Optics.* 36(33):8710–8723.

[55] Rabinowitch, E. I. (1951) Photosynthesis and Related Processes, Vol. II. Part 1. Spectroscopy and Fluorescence of Photosynthetic Pigments; Kinetics of Photosynthesis. Interscience Publishers, New York. 603–671.

[56] Rabinowitch, E. I. (1951) Photosynthesis and Related Processes, Vol. II. Part 1. Spectroscopy and Fluorescence of Photosynthetic Pigments; Kinetics of Photosynthesis. Interscience Publishers, New York. 672–739.

[57] Rosencwaig, A. (1980) Photoacoustics and Photoacoustic Spectroscopy. Wiley, New York.

[58] Rosencwaig, A. and A. Gersho (1976) Theory of the photoacoustic effect with solids. *Journal of Applied Physics.* 47(1):64–69.

[59] Rosencwaig, A. and S. S. Hall (1975) Thin-layer chromatography and photoacoustic spectrometry. *Analytical Chemistry.* 47(3):548–459.

[60] Ruhle, W. and A. Wild (1979) The intensification of absorbance changes in leaves by light-dispersion. *Planta.* 146:551–557.

[61] Salisbury, F. B. and C. Ross (1985) Plant Physiology, 3rd Ed. Wadsworth Publishing, Belmont, California. 183–187.

[62] Seely, G. R. and R. G. Jensen (1965) Effect of solvent on the spectrum of chlorophyll. *Spectrochimica Acta.* 21(10):1835–1845.

[63] Smith, J. H. and A. Benitez (1954) Absorption spectra of chlorophylls. *Yearbook of the Carnegie Institute of Washington.* 168–172.

[64] Stahl, E. (1969) Thin-layer Chromatography: A Laboratory Handbook, 2nd Ed. Springer, New York. 52–85.

[65] Suits, G. (1972) The calculation of the directional reflectance of a vegetative canopy. *Remote Sensing of Environment.* 2:117–125.

[66] Thomas, J. B. (1965) Primary Photoprocesses in Biology. Wiley, New York. 61–153.

[67] Thomas, J. R. and H. W. Gausman (1977) Leaf reflectance vs. leaf chlorophyll and carotenoid concentrations for eight crops. *Agronomy Journal.* 69:799–802.

[68] Thornber, J. P. and J. Barber (1979) Photosynthetic pigments and models for their organization in vivo. *In* Photosyntehsis in relation to model systems. J. Barber, Editor. Elsevier/North-Holland Biomedical Press, Amsterdam. 27–70.

[69] Tucker, C. J., J. H. Elgin Jr., J. E. McMurtrey III, and C. J. Fan (1979) Monitoring corn and soybean crop development with hand-held radiometer spectral data. *Remote Sensing of Environment.* 8:237–248.

[70] Tucker, C. J. and M. W. Garrat (1977) Leaf optical system modeled as stochastic process. *Applied Optics.* 16(3):635–642.

[71] Veeranjaneyulu, K. and V. S. Das (1982) Photoacoustic spectroscopy - leaf absorption spectra. *Journal of Experimental Botany.* 33(134):515–519.

[72] Verhoef, W. (1984) Light scattering by leaf layers with application to reflectance canopy modeling: the SAIL model. *Remote Sensing of Environment.* 16:125–141.

[73] Vogelmann, T. C. (1993) Plant tissue optics. *Annual Review of Plant Physiology and Plant Molecular Biology.* 44:231–251.

[74] Woolley, J. T. (1971) Reflectance and transmittance of light by leaves. *Plant Physiology.* 47(5):656–662.

[75] Yamada, N. and S. Fujimura (1988) A mathematical model of reflectance and transmittance of plant leaves as a function of chlorophyll pigment content. *In* International Geoscience and Remote Sensing Symposium. 833–834.

[76] Zscheile, F. P. and C. L. Comar (1941) Influence of preparative procedure on the purity of chlorophyll components as shown by absorption spectra. *Botanical Gazette.* 102:463–481.

[77] Zscheile, F. P., J. W. White, B. W. Beadle, and J. R. Roach (1942) The preparation and absorption spectra of five pure carotenoid pigments. *Plant Physiology.* 17(3):331–346.

Index

Appendix A

Thin-layer Chromatography

Thin-layer chromatography (TLC) is a powerful yet simple procedure for separating the chemical components of a solution [64, 44, 25]. TLC involves a stationary phase and a liquid phase. The stationary phase is an insoluble adsorbent material, typically silica gel, spread onto an flat sheet of glass or plastic. This is often referred to as the TLC plate. The liquid phase is a solvent containing the solution to be separated.

The technique utilized in TLC for the separation of pigments from a leaf extract can be briefly described as follows. Once the leaf extract has been prepared, usually by mixing crushed leaf material with a solvent such as acetone, a sample is deposited on a TLC plate. The TLC plate is developed by placing it in a beaker filled with a small amount of liquid phase, or solvent. The solvent moves up the plate via capillary action. As the solvent moves over the extract, the pigments will separate

according to how attracted they are to the adsorbent material. Pigments that have a strong affinity will not move very far while those that have a weaker affinity will travel farther up the plate. The end result will be a series of spots at different distances along the TLC plate, with each spot an individual pigment of the leaf extract.

After separation, the pigments can then be removed from the TLC plate using a suitable eluent and light absorption spectroscopy can be performed on the final solution to obtain its light absorption spectrum. Alternatively, photoacoustic absorption spectroscopy can be used to obtain the photoacoustic absorption spectra of the pigments directly from the plates once the developing solvent has evaporated [59]. The ability of photoacousic asbsorption spectroscopy to directly measure from TLC plates without the use of solvent, and its impact on the modeling of leaf optical properties, are discussed in greater detail in Section 4.4.

Appendix B

Approaches for Converting Photoacoustic Absorption Spectra

This appendix presents experimental results comparing the different conversion approaches described in Chapter 3. Light absorption spectra converted from photoacoustic absorption spectra using the intersection point (IP), average (AVG) and minimum (MIN) approach are used to model soybean reflectance (Figure B.1) and transmittance (Figure B.2). Furthermore, the converted light absorption spectra have also been adjusted to account for *in vivo* optical effects, as described in Section 4.3.

Qualitative comparison shows that the light absorption spectra converted using the IP and AVG approach produce modeled spectra that are in close agreement with the measured (LOPEX) curves. In contrast, the light absorption spectra converted

Table B.1: Computed root mean square error (RMSE) values for the modeled soybean spectra using adjusted light absorption spectra converted from photoacoustic absorption spectra. The photocoustic absorption spectra were converted using the intersection point (IP), average (AVG) and minimum (MIN) approach.

	IP	AVG	MIN
reflectance	0.0102	0.0136	0.0188
transmittance	0.0172	0.0162	0.0303

using the MIN approach shows poor agreement. This is particularly noticeable at 500 nm - 600 nm, where the peak of the modeled spectra appears to be much broader and shifted towards the red end of the spectrum.

Quantitative comparison of modeled spectra generated using the IP light absorption spectra produced values that were slightly higher than the measured values, except in the green wavelength range where absorption is minimal. In this wavelength range, around 550 nm, modeled reflectance is slightly lower than the measured values while modeled transmittance shows good agreement. Similarly, the modeled spectra using the AVG light absorption spectra shows good agreement with the measured values from 400 - 500 nm and 580 nm - 700 nm. However, around 550 nm, both the modeled reflectance and transmittance values are lower than both the measured and IP spectral values. Finally, modeled reflectance using the MIN light absorption spectra is in good agreement from 400 - 500 nm, before dropping below measured values. Beyond 575 nm the modeled values are slightly higher. In contrast, the modeled transmittance values are much smaller than the measured values between 400 nm - 570 nm, and then larger from 570 nm - 700 nm.

The tabulated RMSE values (Table B.1) show that the IP conversion approach produced the closest approximation to the reflectance curve, while the AVG approach produced the closest approximation to the transmittance curve. Therefore, both approaches can be treated as suitable candidates for the modeling of leaf optical properties in the visible range. However, the spectral values generated using the IP light absorption spectra were in closer agreement with measured data around the green wavelength range, especially with respect to transmittance. Based on this observation, the IP approach was selected for use in the experiments presented in Chapter 4.

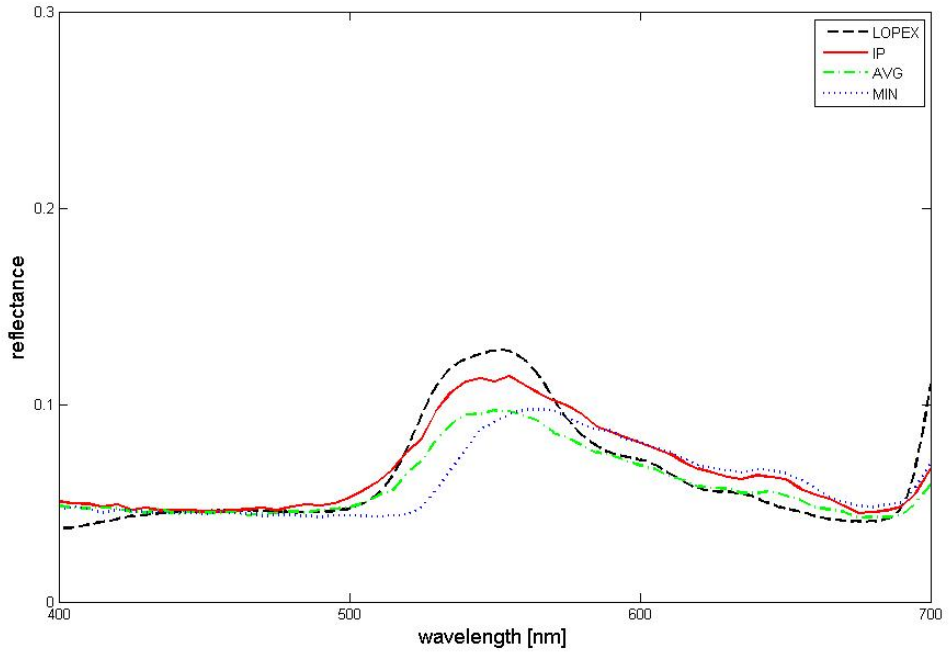

Figure B.1: Comparison between measured (LOPEX) and modeled (ABM-B) *reflectance* curves of soybean leaf (*Glycine max, Soja hispida*). Modeled curves were generated using pigment light absorption spectra converted from photoacoustic absorption spectra using the intersection point (IP), average (AVG) and minimum approach (MIN). The light absorption spectra were multiplied by factors of intensification β (Table 4.4) and shifted 15 nm to account for *in vivo* optical effects.

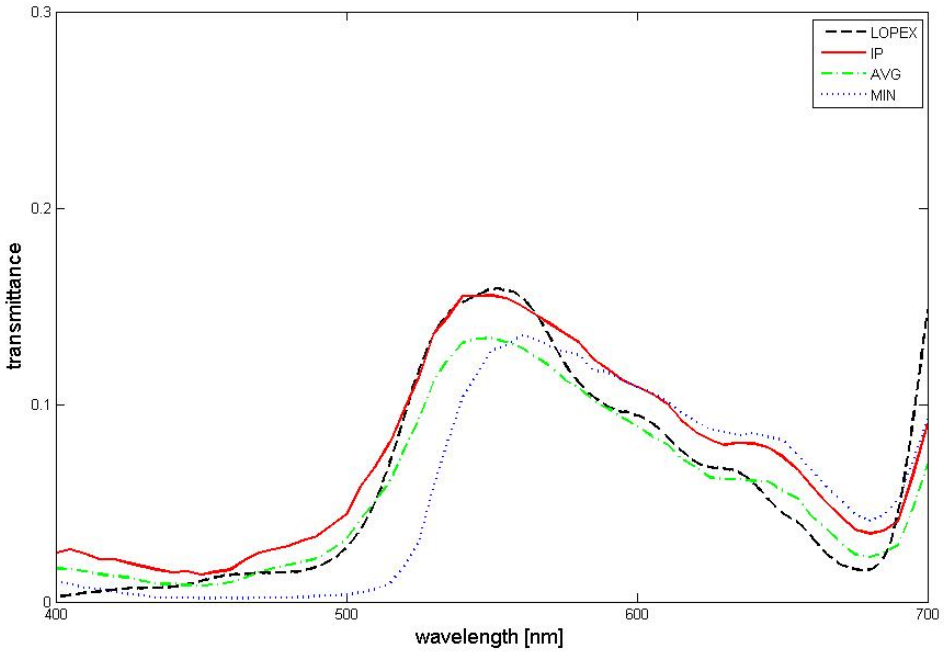

Figure B.2: Comparison between measured (LOPEX) and modeled (ABM-B) *transmittance* curves of soybean leaf (*Glycine max, Soja hispida*). Modeled curves were generated using pigment light absorption spectra converted from photoacoustic absorption spectra using the intersection point (IP), average (AVG) and minimum approach (MIN). The light absorption spectra were multiplied by factors of intensification β (Table 4.4) and shifted 15 nm to account for *in vivo* optical effects.

Appendix C

Estimation of Factor of Intensification

The equations used to estimate the factor of intensification (β) values used in our experiments are provided in Table C.1. The equations take into account β values published by McClendon and Fukshansky [49] and their inverse relationship with respect to pigment concentration [60].

Using the biophysical data in Table 4.1, the pigment concentration[1] is calculated by dividing the pigments' fresh weight by the specimens' area. Based on this calculation, the concentration of chlorophyll a, chlorophyll b and β-carotene is determined to be 33.01 μg/cm^2, 9.64 μg/cm^2 and 9.40 μg/cm^2 respectively. Ap-

[1]Pigment concentration with respect to β values is expressed as weight per area (g/cm^2), not weight per volume (g/cm^3). Alternatively, some researchers may use the term pigment density instead of pigment concentration when describing the correlation between pigment content and β values.

Table C.1: Linear equations relating the chlorophyll concentration (c) with the factor of intensification (β) [49, 60].

Chlorophyll concentration range (μg/cm^2)	Factor of Intensification (β)
20-40	3.59 - 0.028c
13-20	7.58 - 0.220c

plying the equations given in Table C.1, the β values estimated for chlorophyll a, chlorophyll b and β-carotene are 2.67, 5.46 and 5.51 respectively.

The factors of intensification used to formulate the equations given in Table C.1 are based on extrapolated values of leaf transmittance at the red end of the spectrum (665 nm - 690 nm). However, as observed by Ruhle and Wild, β values change according to wavelength: based on measurements for seven plant species, β values ranged from 0.90-1.70 at 680 nm, and 2.04-2.69 at 554 nm [60]. Therefore in order to model leaf optical properties across the entire visible range (400 nm - 700 nm), the β values are adjusted to be slightly lower than calculated.

The ratio of the β value for chlorophyll b with respect to chlorophyll a is 1:2.04 and the ratio for β-carotene is 1:2.06. Using these ratios with a lowered β value of 2.0 for chlorophyll a, the β value for both chlorophyll b and β-carotene is determined to be 4.1. These are the factors of intensification used in our experiments, as presented in Table 4.4.